Tomographic Imaging with Model Uncertainty

Low-Rank Models and Applications, June 9-11, 2021

Martin S. Andersen

Section for Scientific Computing

Department of Applied Mathematics and Compute Science

Technical University of Denmark (DTU)

joint work with Katrine Ottesen Bangsgaard

X-ray computed tomography

Projection images

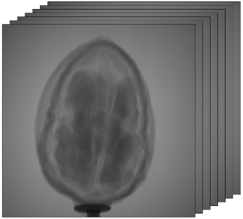

X-ray computed tomography

Projection images

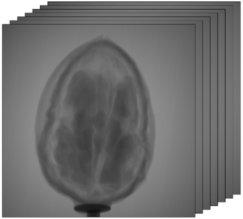

Flat-field image

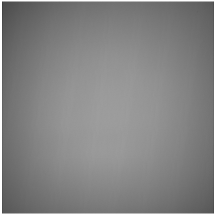

X-ray computed tomography

Projection images

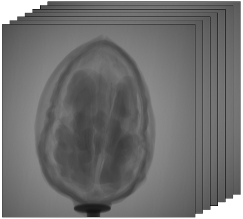

Flat-field image

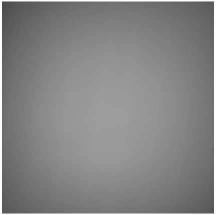

Transmission images

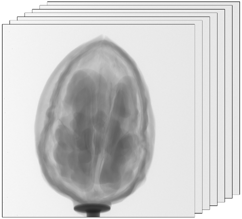

X-ray computed tomography

Projection images

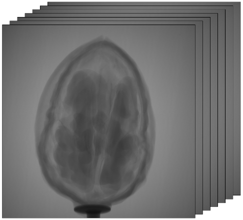

Flat-field image

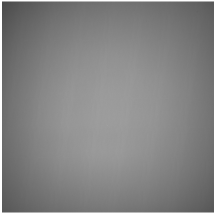

Transmission images

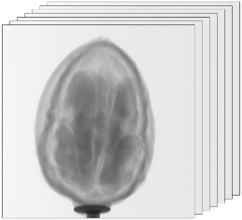

Transmission sinogram

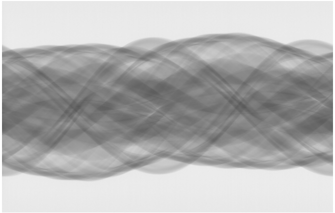

X-ray computed tomography

Projection images

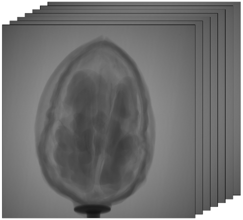

Flat-field image

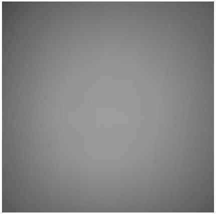

Transmission images

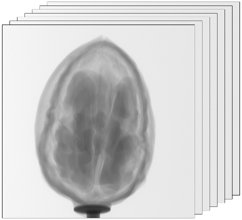

Transmission sinogram

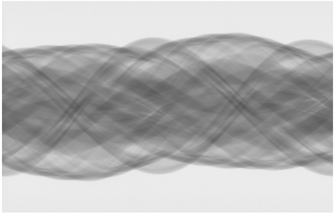

Attenuation image

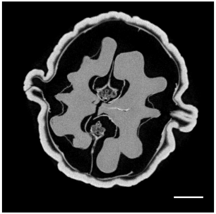

Lambert–Beer's law

$$-\log(I_i/I_0) = \int_{l_i} \mu(x)\, ds$$

$$b_i \approx a_i^T u$$

$$b = Au + e$$

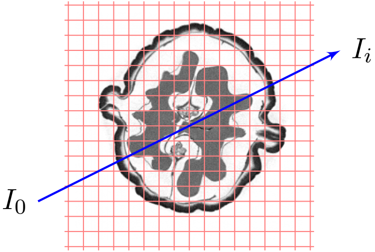

Parallel beam measurement geometry

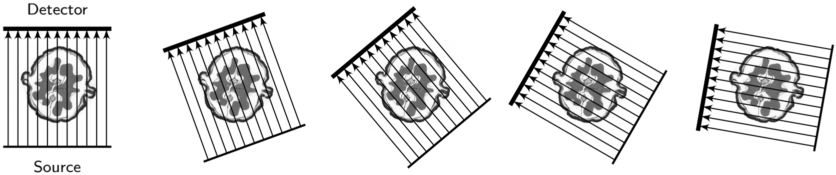

Reconstruction methods

- Analytic methods (inverse Radon transform, FBP, gridrec)
- Algebraic methods (Kaczmarz, ART, Cimmino, SIRT, CGLS, ...)

$$Au \approx b$$

- Variational methods (ML, MAP, ...)

$$\text{minimize} \quad \tfrac{1}{2}\|Au - b\|_W^2 + \gamma\, h(u)$$

Noisy X-ray images (low dose / fast acquisition)

Projection images

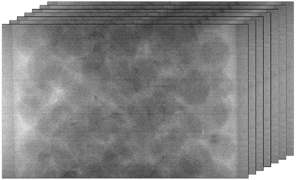

Flat-field image

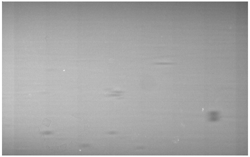

Transmission images

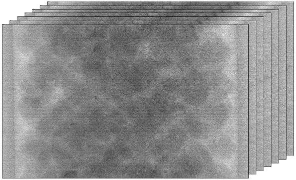

Noisy X-ray images (low dose / fast acquisition)

Projection images

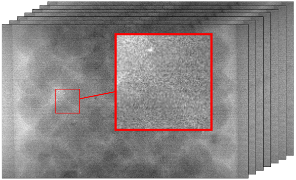

Flat-field image

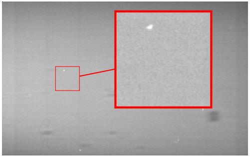

Transmission images

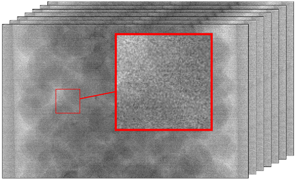

Noisy X-ray images (low dose / fast acquisition)

Projection images

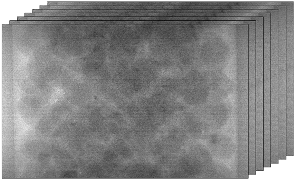

Flat-field image

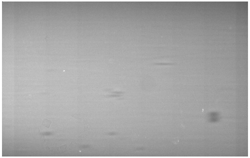

Transmission images

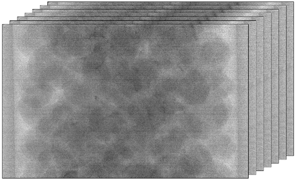

Transmission sinogram

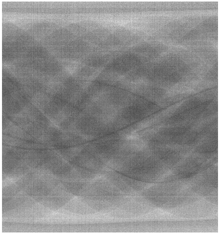

2D reconstruction

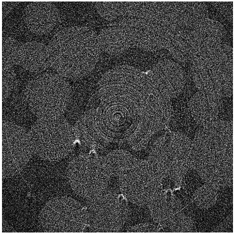

Ring artifacts

Transmission sinogram (1)

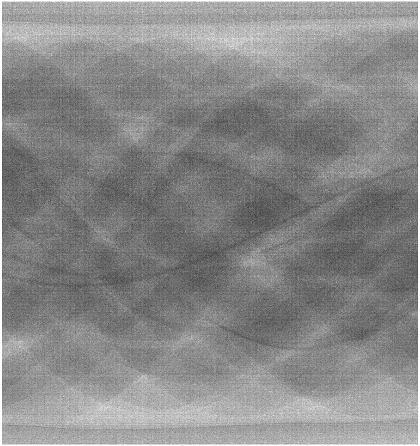

2D reconstruction (1)

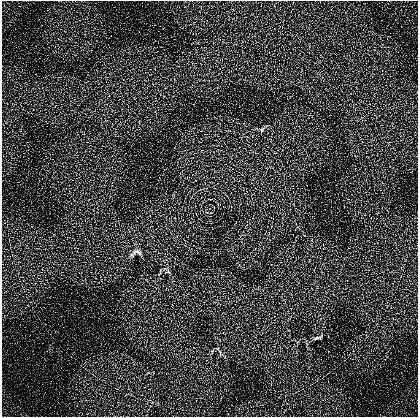

Ring artifacts

Transmission sinogram (3)

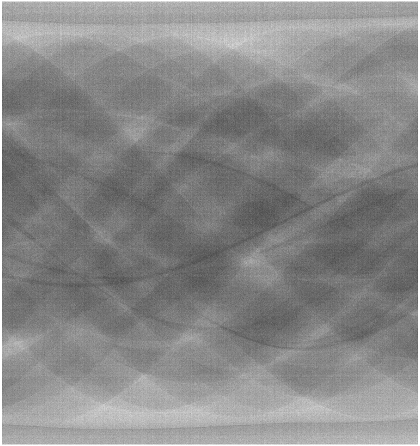

2D reconstruction (3)

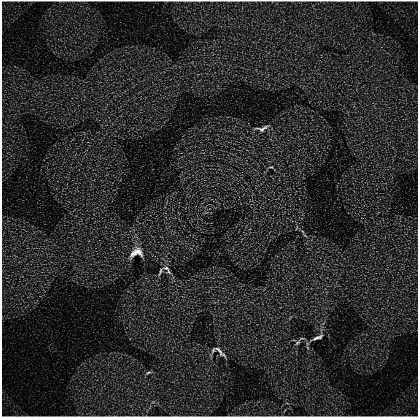

Ring artifacts

Transmission sinogram (5)

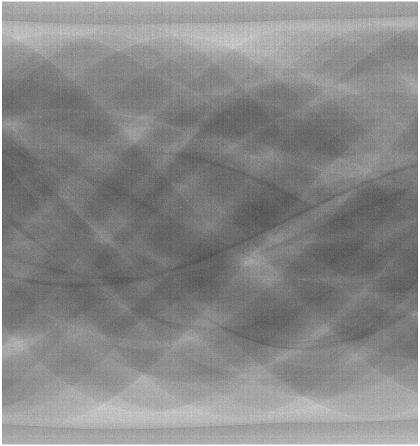

2D reconstruction (5)

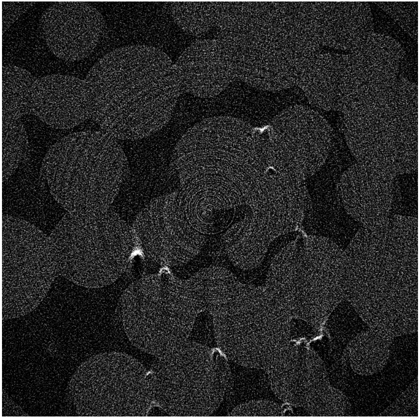

Ring artifacts

Transmission sinogram (11)

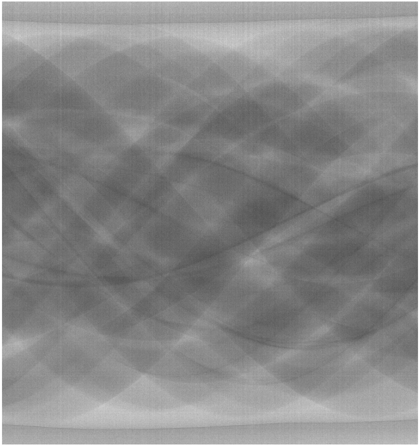

2D reconstruction (11)

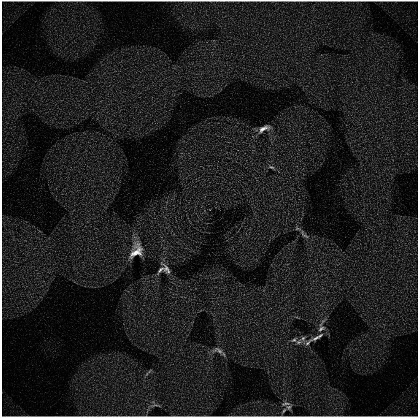

Flat-field errors

A flat-field estimation error shows up as a ring in the reconstruction

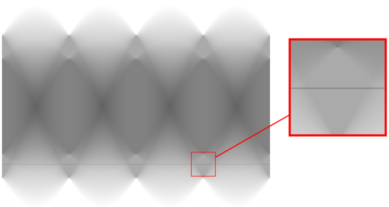

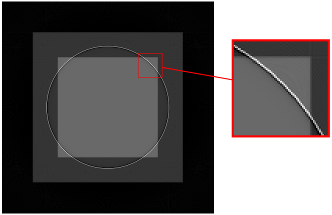

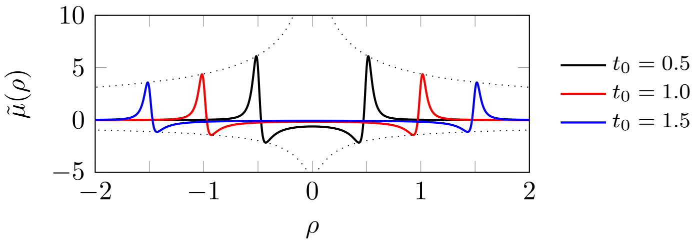

Related work

- preprocessing (stripe-removal) [Kow78, Rav98, MTMS09, RLH12, KBH14, VAD18]
- post-reconstruction processing (ring-removal) [SP04, PKK09, YWZZ16]
- part of reconstruction [PM15, MVG$^+$15, AARS18, SWG$^+$19]

$$\text{minimize} \quad \tfrac{1}{2}\|Au - b + \mathbf{1}\otimes z\|_2^2 + \gamma\, h(z) + \delta\, g(u)$$

motivated by measurement model $y \sim \mathrm{Poisson}\left(I_0\, \mathbf{diag}(\mathbf{1}\otimes\nu)\exp(-Au)\right)$

$$Au \simeq -\log(y) + \mathbf{1}\otimes\log(\hat{\nu}) = \bar{b} + e + \mathbf{1}\otimes z = b, \quad z_i \sim \mathcal{N}(0, 1/(sI_0\nu_i))$$

- acquisition: time-delay integration [DE97], object/detector shifts [ZZLZ13]

Related work

- preprocessing (stripe-removal) [Kow78, Rav98, MTMS09, RLH12, KBH14, VAD18]
- post-reconstruction processing (ring-removal) [SP04, PKK09, YWZZ16]
- part of reconstruction [PM15, MVG+15, AARS18, SWG+19]

$$\text{minimize} \quad \tfrac{1}{2}\|Au - b + \mathbf{1} \otimes z\|_2^2 + \gamma\, h(z) + \delta\, g(u)$$

motivated by measurement model $y \sim \mathrm{Poisson}\,(I_0\, \mathbf{diag}(\mathbf{1} \otimes \nu)\exp(-Au))$

$$Au \simeq -\log(y) + \mathbf{1} \otimes \log(\hat{\nu}) = \bar{b} + e + \mathbf{1} \otimes z = b, \qquad z_i \sim \mathcal{N}(0, 1/(sI_0\nu_i))$$

- acquisition: time-delay integration [DE97], object/detector shifts [ZZLZ13]

FBP($\bar{b}$) FBP(e) FBP($\mathbf{1} \otimes z$) FBP(Sz)

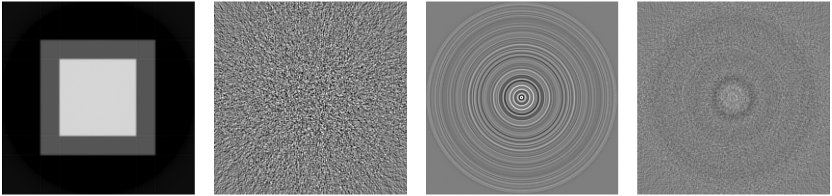

Related work

- preprocessing (stripe-removal)
  [Kow78, Rav98, MTMS09, RLH12, KBH14, VAD18]
- post-reconstruction processing (ring-removal) [SP04, PKK09, YWZZ16]
- part of reconstruction [PM15, MVG$^+$15, AARS18, SWG$^+$19]

$$\text{minimize} \quad \tfrac{1}{2}\|Au - b + \mathbf{1} \otimes z\|_2^2 + \gamma\, h(z) + \delta\, g(u)$$

  motivated by measurement model $y \sim \mathrm{Poisson}\left(I_0\, \mathbf{diag}(\mathbf{1} \otimes \nu)\exp(-Au)\right)$

$$Au \simeq -\log(y) + \mathbf{1} \otimes \log(\hat{\nu}) = \bar{b} + e + \mathbf{1} \otimes z = b, \quad z_i \sim \mathcal{N}(0, 1/(sI_0\nu_i))$$

- acquisition: time-delay integration [DE97], object/detector shifts [ZZLZ13]
- this talk: joint estimation of intensity, detector response and attenuation image

Motivation

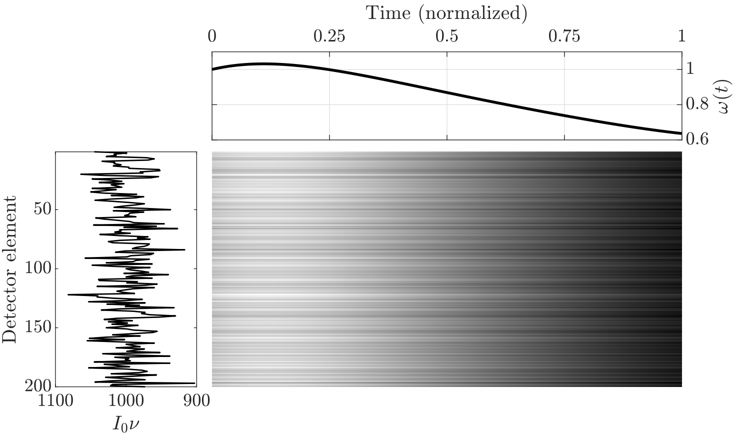

Neutron tomography: low signal-to-noise ratio, time-varying intensity

Connection to matrix completion

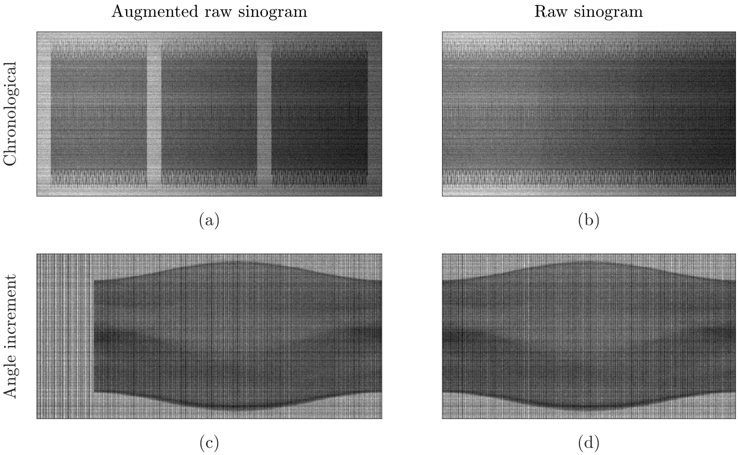

Extended model

Model uncertainty: detector response and time-varying intensity

$$I_i(t_j,\theta_j) = I_0\,\nu_i\,\omega_j \exp\left(-\delta_j \int_{\ell_i(\theta_j)} \mu(x)\,dx\right), \quad i = 1,\dots,r,$$

$$\overline{Y}(U, I_0, \nu, \omega) = I_0(\nu\omega^T) \circ \exp\left(-\mathcal{A}(U)\right)$$

Change of variables

$$I_0\nu = \mathbf{diag}(\hat{\nu})\exp(-v), \quad \omega = \mathbf{diag}(\hat{\omega})\exp(-w),$$

yields

$$\bar{y}(u, v, w; \hat{\nu}, \hat{\omega}) = \mathbf{diag}(\hat{\omega} \otimes \hat{\nu})\exp(-Au - \mathbf{1} \otimes v - w \otimes \mathbf{1}),$$

Measurement model

Poisson measurements (photon counts)

$$y|u, v, w, \hat{\nu}, \hat{\omega} \sim \mathrm{Poisson}(\bar{y})$$

- $\hat{\nu}$ (and sometimes also $\hat{\omega}$) can be estimated from flat-field images
- negative log-likelihood

$$-\log(\pi(y|u, v, w)) = \mathbf{1}^T \bar{y} - y^T \log(\bar{y}) + \mathbf{1}^T \log(y!)$$

- maximum a posteriori estimation

$$\pi(u, v, w|y) \propto \pi(y|u, v, w)\pi(u, v, w)$$

- quadratic approximation

$$\frac{1}{2}\|Au + \mathbf{1} \otimes v + w \otimes \mathbf{1} - b\|_W^2 + \gamma\, h(u, v, w), \quad b = \log(\hat{\omega} \otimes \hat{\nu}) - \log(y)$$

Methodology

1. Compute $\hat{\nu}$ from flat-field samples f

$$\hat{\nu} = \underset{\nu}{\operatorname{argmax}}\{\pi(f|\nu, \omega = \mathbf{1})\}$$

2. Compute $\hat{\omega} = \omega(\hat{\alpha})$

$$\hat{\alpha} = \underset{\alpha}{\operatorname{argmax}}\{\pi(f|\hat{\nu}, \omega(\alpha))\}$$

3. Compute point estimates, credible intervals, etc., from posterior distribution

$$\pi(u, v, w, \eta|y, \hat{\nu}, \hat{\omega}) \propto \pi(y|u, v, w)\pi(u, v, w|\eta)\pi(\eta)$$

Numerical results (I)

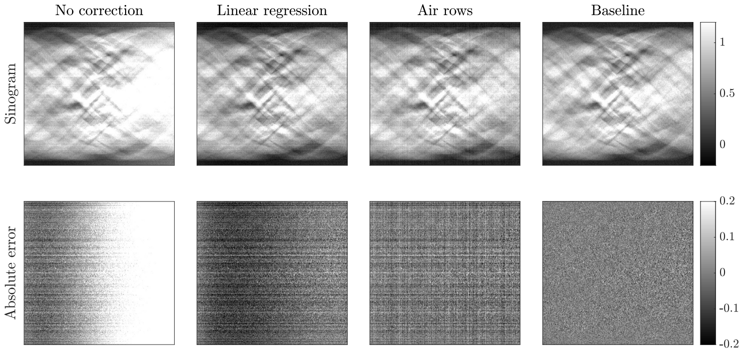

Numerical results (I)

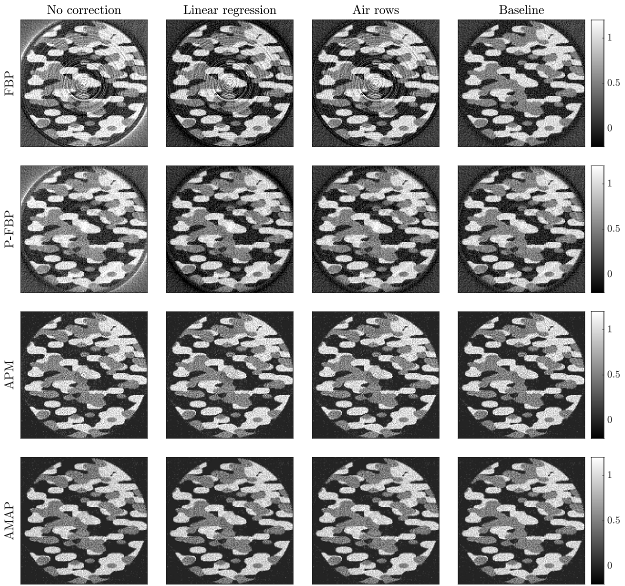

Numerical results (I)

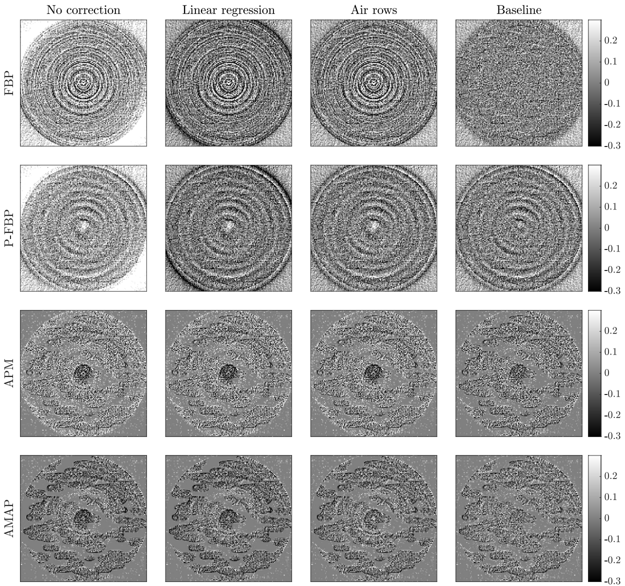

Numerical results (II)

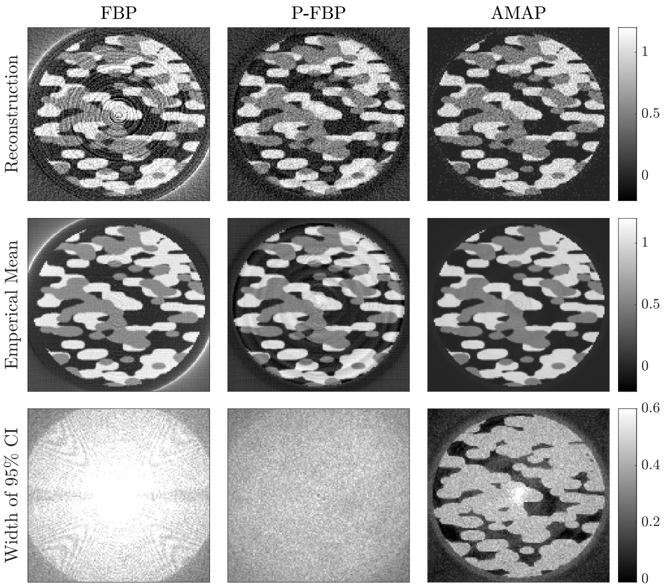

Numerical results (II)

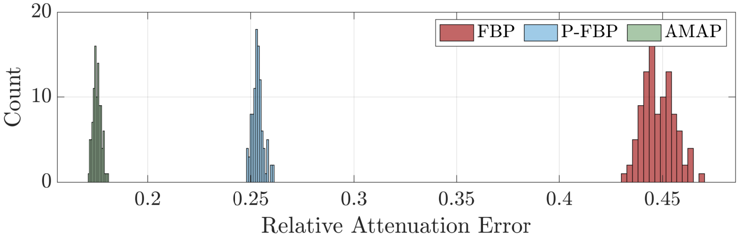

Extensions

- low-rank source-detector model

$$\bar{y} = \mathbf{diag}(\mathrm{vec}(Z))\exp(-Au), \quad Z \approx VW^T$$

- spectral CT

$$I_{i,k}(\theta, t) = \int_0^E I_0(e)\nu_{i,k}(e)\omega(t)\exp\left(-\int_{l_i(\theta)} \mu(x,e)\,dx\right) de$$

- estimate $\hat{\omega}$ via smoothing spline regression [AC20]

$$\omega(\alpha) = \Sigma\alpha \quad \text{where} \quad \Sigma = \Sigma^T,\ \mathbf{tril}(\Sigma) = \mathbf{tril}(AB^T)$$

Summary

- new extended reconstruction model that includes source-detector uncertainty
- joint estimation of rank-1 matrix and attenuation image
- useful for low-intensity experiments (e.g., low dose / fast acquisition)

Thank you for listening!

References I

H. O. Aggrawal, M. S. Andersen, S. Rose, and E. Y. Sidky, *A convex reconstruction model for x-ray tomographic imaging with uncertain flat-fields*, IEEE Transactions on Computational Imaging **4** (2018), no. 1, 17–31.

M. S. Andersen and T. Chen, *Smoothing splines and rank structured matrices: Revisiting the spline kernel*, SIAM Journal on Matrix Analysis and Applications **42** (2020), no. 2, 389–412.

G. R Davis and J. C Elliott, *X-ray microtomography scanner using time-delay integration for elimination of ring artefacts in the reconstructed image*, Nuclear Instruments and Methods in Physics Research Section A: Accelerators, Spectrometers, Detectors and Associated Equipment **394** (1997), no. 1-2, 157–162.

T. Kim, J. Baek, and D. Hwang, *Ring artifact correction using detector line-ratios in computed tomography*, Opt. Express **22** (2014), no. 11, 13380–92.

G. Kowalski, *Suppression of ring artefacts in CT Fan-Beam scanners*, IEEE Trans. Nucl. Sci. **25** (1978), no. 5, 1111–1116.

B. Münch, P. Trtik, F. Marone, and M. Stampanoni, *Stripe and ring artifact removal with combined wavelet—Fourier filtering*, Opt. Express **17** (2009), no. 10, 8567.

References II

K. A. Mohan, S. V. Venkatakrishnan, J. W. Gibbs, E. B. Gulsoy, X. Xiao, M. De Graef, P. W. Voorhees, and C. A. Bouman, *TIMBIR: A method for time-space reconstruction from interlaced views*, IEEE Trans. Comput. Imaging **1** (2015), no. 2, 96–111.

D. Prell, Y. Kyriakou, and W. A Kalender, *Comparison of ring artifact correction methods for flat-detector CT.*, Phys. Med. Biol. **54** (2009), no. 12, 3881–95.

P. Paleo and A. Mirone, *Ring artifacts correction in compressed sensing tomographic reconstruction.*, J. Synchrotron Radiat. **22** (2015), no. 5, 1268–78.

C. Raven, *Numerical removal of ring artifacts in microtomography*, Rev. Sci. Instrum. **69** (1998), no. 8, 2978.

S. Rashid, S Lee, and M. Hasan, *An improved method for the removal of ring artifacts in high resolution CT imaging*, EURASIP J. Adv. Signal Process. **2012** (2012), no. 1, 93.

J. Sijbers and A. Postnov, *Reduction of ring artefacts in high resolution micro-CT reconstructions.*, Phys. Med. Biol. **49** (2004), no. 14, N247–53.

References III

M. Salehjahromi, Q. Wang, L. A. Gjesteby, D. Harrison, G. Wang, and H. Yu, *A directional TV based ring artifact reduction method*, Medical Imaging 2019: Physics of Medical Imaging (Hilde Bosmans, Guang-Hong Chen, and Taly Gilat Schmidt, eds.), SPIE, March 2019.

N. T. Vo, R. C. Atwood, and M. Drakopoulos, *Superior techniques for eliminating ring artifacts in x-ray micro-tomography*, Optics Express **26** (2018), no. 22, 28396.

L. Yan, T. Wu, S. Zhong, and Q. Zhang, *A variation-based ring artifact correction method with sparse constraint for flat-detector CT.*, Phys. Med. Biol. **61** (2016), no. 3, 1278–92.

Y. Zhu, M. Zhao, H. Li, and P. Zhang, *Micro-CT artifacts reduction based on detector random shifting and fast data inpainting*, Medical Physics **40** (2013), no. 3, 031114.

Martin S. Andersen
Department of Applied Mathematics and Computer Science
Technical University of Denmark (DTU)

Building 303B, Room 113
2800 Kgs. Lyngby, Denmark
http://people.compute.dtu.dk/mskan

mskan@dtu.dk
+45 45253036 phone